Advances in Applied Mathematics and Mechanics
Adv. Appl. Math. Mech., Vol. **6**, No. 5, pp. 539-551

DOI: 10.4208/aamm.2013.m360
October 2014

Stability of Atomic Simulations with Matching Boundary Conditions

Shaoqiang Tang* and Songsong Ji

HEDPS, CAPT and LTCS, College of Engineering, Peking University, Beijing 100871, China

Received 27 September 2013; Accepted (in revised version) 21 February 2014

Available online 23 June 2014

Abstract. We explore the stability of matching boundary conditions in one space dimension, which were proposed recently for atomic simulations (Wang and Tang, Int. J. Numer. Mech. Eng., 93 (2013), pp. 1255–1285). For a finite segment of the linear harmonic chain, we construct explicit energy functionals that decay along with time. For a nonlinear atomic chain with its nonlinearity vanished around the boundaries, an energy functional is constructed for the first order matching boundary condition. Numerical verifications are also presented.

AMS subject classifications: 70-08, 65L99, 34B60

Key words: Stability, matching boundary condition, atomic simulation.

1 Introduction

Atomic and multiscale computations are widely used in materials science and engineering, where the atomic dynamics are resolved only over a subdomain much smaller than the complete underlying systems [8]. As artificial boundaries are introduced numerically, spurious wave reflections may appear, propagate backward and corrupt the local physics. Effective boundary or interfacial conditions are thus crucial for fidel simulations. A class of time history treatments provide exact conditions in linear lattices, yet convolutions cause heavy computing load and considerably reduce the efficiency [1–3, 13, 14, 17]. In addition, they are not exact and sometimes even not applicable for nonlinear lattices, and the kernel functions in a finite computing domain are difficult to obtain in multiple dimensions [9]. In view of these complexities, local approximate boundary treatments

*Corresponding author.
Email: maotang@pku.edu.cn (S. Q. Tang), songsong.0211@163.com (S. S. Ji)

have been proposed, such as the perfect matched layer method [10, 16], the velocity interfacial conditions [11], and the matching boundary conditions [18]. While the effectiveness for these treatments has been demonstrated numerically, rigorous mathematical proof for the stability are widely open, except for a lowest order velocity interfacial condition [4, 11]. We notice that a semi-discrete finite difference scheme of a wave equation shares the same form with the dynamical equations for atomic chains. For such a scheme, there are studies on stability for boundary treatments, such as the Gustafsson-Kreiss-Sundström theory. However, this theory is based on a wave view for semi-infinite domain, hence only one-sided boundary conditions have been treated [15]. It does not apply to a finite segment of an atomic chain in general. In fact, stability of a finite segment can be a delicate issue, and stability for semi-infinite chain may not imply that for a finite segment [12].

In this work, we establish the stability for several matching boundary conditions on a finite segment of an atomic chain. This class of boundary conditions were proposed by matching the dispersion relation of a linear lattice. They are local in both space and time, hence allow extension to nonlinear lattices by local linearization. Furthermore, for multiple dimensions, the square, triangular, face-centered-cubic and body-centered-cubic lattices have been successfully treated through operator multiplication of such conditions at several selected incident angles [5, 6, 18]. Numerical tests and applications have verified the effectiveness, with reflections well suppressed. For MBC1, MBC2 and MBC3 shown in the next section, we construct energy functionals that decay along with time. These energies, as we shall see afterwards, induce semi-norms. Up to a linear dilation, the atomic chain with these boundary conditions equilibrates. Stability of MBC1 is also established for a nonlinear chain.

The rest of this paper is organized as follows. In Section 2, we describe these matching boundary conditions. Energy functionals for the linear lattice are constructed and verified in Section 3. An energy functional is constructed in Section 4 for nonlinear chains. Some concluding remarks are made in Section 5.

2 Matching boundary conditions

We consider a one-dimensional chain with nearest neighbor interaction. For the k-th atom, its displacement away from equilibrium is denoted by $u_k(t)$. The total potential of the chain consists of pair-wise potentials $J_{l+1/2}(u_{l+1}-u_l)$. With a uniform mass m, the dynamics is governed by the Newton equations.

$$m\ddot{u}_k = -\nabla_{u_k}\Big[\sum_l J_{l+1/2}(u_{l+1}-u_l)\Big] = J'_{k+1/2}(u_{k+1}-u_k) - J'_{k-1/2}(u_k-u_{k-1}), \quad k\in\mathbb{Z}. \tag{2.1}$$

For a harmonic chain, we have $J_{l+1/2}(u_{l+1}-u_l)=\kappa(u_{l+1}-u_l)^2/2$, where κ is the elastic constant. Hence the Newton equations read

$$m\ddot{u}_k = \kappa(u_{k+1}-2u_k+u_{k-1}), \quad k\in\mathbb{Z}. \tag{2.2}$$

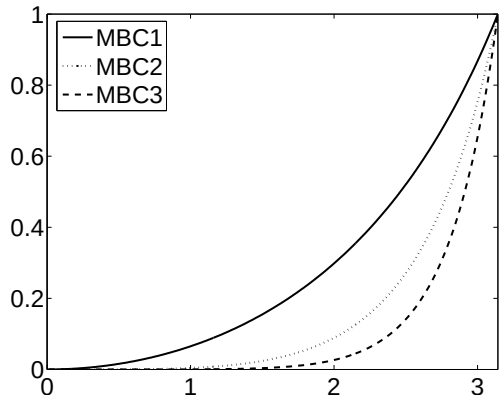

Figure 1: Reflection coefficients for matching boundary conditions. The horizontal axis represents the wave number, and the vertical axis represents the reflection coefficient.

We rescale time by $\sqrt{m/\kappa}$, and recast the system into

$$\ddot{u}_k = u_{k+1} - 2u_k + u_{k-1}, \quad k \in \mathbb{Z}. \tag{2.3}$$

Consider an atomic computing domain Ω that contains the atoms $k=-N,\cdots,N$. We illustrate the construction of the matching boundary conditions (MBC) at the right boundary u_N as follows.

A monochromatic right-going wave at a wave number $\xi \in [0,\pi]$ takes the form of $u_k(t) \sim e^{i(\omega t - \xi k)}$, where the frequency is dictated by the dispersion relation

$$\omega = 2\sin\frac{\xi}{2}. \tag{2.4}$$

A matching boundary condition relates the displacements and velocities near the boundary in a linear form.

$$\sum_{p=0}^{P} c_p \dot{u}_{N-p} - \sum_{p=0}^{P} b_p u_{N-p} = 0. \tag{2.5}$$

Substituting the wave form into the left hand side and discard the common factor, we define a matching residual function

$$\Delta(\xi) = i\omega(\xi) \sum_{p=0}^{P} c_p e^{i\xi p} - \sum_{p=0}^{P} b_p e^{i\xi p}. \tag{2.6}$$

This residual function measures the inconsistency for imposing the linear relation (2.5) on a right-going wave. For a particular choice of parameters $\{b_1,\cdots,b_P,c_1,\cdots,c_P\}$, transparent transmission is reached at a certain wave number if the residual function vanishes there. Obviously such ideal transmission can not hold over the positive half interval of the first Brillouin zone $[0,\pi]$. As long waves usually dominate the energy band,

a class of Taylor type MBC's were explicitly formulated by enforcing $\Delta(\xi)=o(\xi^P)$ [18]. The first three of them are as follows:

$$\dot{u}_N+\dot{u}_{N-1}=2(-u_N+u_{N-1}), \tag{2.7a}$$
$$\dot{u}_N+6\dot{u}_{N-1}+\dot{u}_{N-2}=4(-u_N+u_{N-2}), \tag{2.7b}$$
$$\dot{u}_N+15\dot{u}_{N-1}+15\dot{u}_{N-2}+\dot{u}_{N-3}=-6u_N-14u_{N-1}+14u_{N-2}+6u_{N-3}. \tag{2.7c}$$

The suppression of reflection waves is progressively enhanced when the order of MBC increases. See the reflection coefficients in Fig. 1.

3 Energy functionals for harmonic chain

For the linear harmonic chain (2.3), we start with some elemental functionals. Then we construct energy functionals to establish stability results for the afore-mentioned conditions (2.7a)-(2.7c), respectively.

3.1 Energy functionals

We start with several energy functionals as follows.

$$I_1(K)=\frac{1}{2}\Big[\sum_{k=-K+1}^{K-1}\dot{u}_k^2+\sum_{k=-K+1}^{K}(u_k-u_{k-1})^2\Big], \tag{3.1a}$$
$$I_2(K)=\frac{1}{2}\Big[\sum_{k=-K+2}^{K-1}(\dot{u}_k+\dot{u}_{k-1})^2+\sum_{k=-K+2}^{K}(u_k-u_{k-2})^2\Big], \tag{3.1b}$$
$$I_3(K)=\frac{1}{2}\Big[\sum_{k=-K+3}^{K-1}(\dot{u}_k+\dot{u}_{k-2})^2+\sum_{k=-K+3}^{K}(u_k-u_{k-1}+u_{k-2}-u_{k-3})^2\Big]. \tag{3.1c}$$

Each functional is non-negative, and may induce a semi-norm in the state space. Moreover, all summands are symmetric with respect to atomic indices.

Making use of the Newton equations, we calculate the derivative of $I_1(K)$ as follows.

$$\begin{aligned}\dot{I}_1(K)&=\sum_{k=-K+1}^{K-1}\dot{u}_k(u_{k-1}-2u_k+u_{k+1})+\sum_{k=-K+1}^{K}(\dot{u}_k-\dot{u}_{k-1})(u_k-u_{k-1})\\&=\sum_{k=-K+1}^{K-1}\dot{u}_k(u_{k-1}-2u_k+u_{k+1})+\sum_{k=-K+1}^{K}\dot{u}_k(u_k-u_{k-1})+\sum_{k=-K}^{K-1}\dot{u}_k(u_k-u_{k+1})\\&=\dot{u}_K(u_K-u_{K-1})+n.b.t..\end{aligned}$$

Here, $n.b.t.=\dot{u}_{-K}(u_{-K}-u_{-K+1})$. In the sequel, we use $n.b.t.$ to denote the negative boundary term(s), which is symmetric with respect to K.

In a similar fashion, we calculate

$$\begin{aligned}
\dot{I}_2(K) &= \sum_{k=-K+2}^{K-1} (\dot{u}_k+\dot{u}_{k-1})(u_{k-2}-u_{k-1}-u_k+u_{k+1}) + \sum_{k=-K+2}^{K} (\dot{u}_k-\dot{u}_{k-2})(u_k-u_{k-2}) \\
&= \sum_{k=-K+2}^{K-1} \dot{u}_k(u_{k-2}-u_{k-1}-u_k+u_{k+1}) + \sum_{k=-K+1}^{K-2} \dot{u}_k(u_{k-1}-u_k-u_{k+1}+u_{k+2}) \\
&\quad + \sum_{k=-K+2}^{K} \dot{u}_k(u_k-u_{k-2}) + \sum_{k=-K}^{K-2} \dot{u}_k(u_k-u_{k+2}) \\
&= (\dot{u}_K+\dot{u}_{K-1})(u_K-u_{K-2}) + n.b.t., \\
\dot{I}_3(K) &= \sum_{k=-K+3}^{K-1} (\dot{u}_k+\dot{u}_{k-2})(u_{k-3}-2u_{k-2}+2u_{k-1}-2u_k+u_{k+1}) \\
&\quad + \sum_{k=-K+3}^{K} (\dot{u}_k-\dot{u}_{k-1}+\dot{u}_{k-2}-\dot{u}_{k-3})(u_k-u_{k-1}+u_{k-2}-u_{k-3}) \\
&= \sum_{k=-K+3}^{K-1} \dot{u}_k(u_{k-3}-2u_{k-2}+2u_{k-1}-2u_k+u_{k+1}) \\
&\quad + \sum_{k=-K+1}^{K-3} \dot{u}_k(u_{k-1}-2u_k+2u_{k+1}-2u_{k+2}+u_{k+3}) \\
&\quad + \sum_{k=-K+3}^{K} \dot{u}_k(u_k-u_{k-1}+u_{k-2}-u_{k-3}) + \sum_{k=-K+2}^{K-1} \dot{u}_k(-u_{k+1}+u_k-u_{k-1}+u_{k-2}) \\
&\quad + \sum_{k=-K+1}^{K-2} \dot{u}_k(u_{k+2}-u_{k+1}+u_k-u_{k-1}) + \sum_{k=-K}^{K-3} \dot{u}_k(-u_{k+3}+u_{k+2}-u_{k+1}+u_k) \\
&= (\dot{u}_K+\dot{u}_{K-2})(u_K-u_{K-1}+u_{K-2}-u_{K-3}) + n.b.t..
\end{aligned}$$

We remark that the above energy functionals suggest the following stable and dissipative boundary conditions.

$$\dot{u}_N = \alpha(u_{N-1}-u_N), \tag{3.2a}$$

$$\dot{u}_N+\dot{u}_{N-1} = \beta(u_{N-2}-u_N), \tag{3.2b}$$

$$\dot{u}_N+\dot{u}_{N-2} = \gamma(u_{N-3}-u_{N-2}+u_{N-1}-u_N). \tag{3.2c}$$

Here, α, β, γ are arbitrary positive constants. The condition (3.2a) gives the velocity interfacial condition if $\alpha=1$ is chosen [11].

Next, we express each following term as the sum of a complete derivative and terms in $\dot{I}_l(K)$, $(l=1,2,3)$.

$$\dot{u}_K u_{K-1} = -\dot{u}_K(u_K-u_{K-1}) + \Big(\frac{u_K^2}{2}\Big)^{\cdot}, \tag{3.3a}$$

$$\dot{u}_K u_{K-2} = -(\dot{u}_K+\dot{u}_{K-1})(u_K-u_{K-2})+\dot{u}_K(u_K-u_{K-1}) \\ +\dot{u}_{K-1}(u_{K-1}-u_{K-2})+\Big(u_K u_{K-1}-\frac{u_{K-1}^2}{2}\Big)^{\cdot}, \tag{3.3b}$$

$$\dot{u}_K u_{K-3} = -(\dot{u}_K+\dot{u}_{K-2})(u_K-u_{K-1}+u_{K-2}-u_{K-3})+\dot{u}_K(u_K-u_{K-1}) \\ -\dot{u}_{K-1}(u_{K-1}-u_{K-2})+\dot{u}_{K-2}(u_{K-2}-u_{K-3}) \\ +\Big(\frac{u_{K-1}^2}{2}+u_K u_{K-2}-u_{K-1}u_{K-2})\Big)^{\cdot}. \tag{3.3c}$$

3.2 Energy functional for MBC1

Based on the above functionals, we construct a suitable linear combination of them, and add some boundary terms to form a new functional. The new functional is expected to decay along with time under the proposed boundary conditions. In particular, for MBC1 (2.7a), we calculate the product of its left and right hand sides.

$$\begin{aligned}&(\dot{u}_N+\dot{u}_{N-1})(u_N-u_{N-1})\\ =&-2\dot{u}_N u_{N-1}+\dot{u}_N u_N-\dot{u}_{N-1}u_{N-1}+(u_N u_{N-1})^{\cdot}\\ =&2\dot{u}_N(u_N-u_{N-1})-\frac{1}{2}[(u_N-u_{N-1})^2]^{\cdot}.\end{aligned}$$

Noticing the form of I_1, we define an energy functional

$$E_1(t)=\sum_{k=-N+1}^{N-1}\dot{u}_k^2+\sum_{k=-N+2}^{N-1}(u_k-u_{k-1})^2+\frac{1}{2}(u_{-N}-u_{-N+1})^2+\frac{1}{2}(u_N-u_{N-1})^2. \tag{3.4}$$

We have

$$\dot{E}_1(t)=-2(u_N-u_{N-1})^2-2(u_{-N}-u_{-N+1})^2\le 0. \tag{3.5}$$

This proves that $E_1(t)$ is a non-negative energy functional for MBC1, which decreases along with time.

3.3 Energy functional for MBC2

For MBC2 (2.7b), similar calculations are performed. Multiplying the two sides of (2.7b), we express the product with full derivatives and afore-mentioned terms in $\dot{I}_l(K)$.

$$\begin{aligned}&(\dot{u}_N+6\dot{u}_{N-1}+\dot{u}_{N-2})(u_N-u_{N-2})\\ =&-6\dot{u}_N u_{N-1}-2\dot{u}_N u_{N-2}-6\dot{u}_{N-1}u_{N-2}+\dot{u}_N u_N-\dot{u}_{N-2}u_{N-2}+(6u_N u_{N-1}+u_N u_{N-2})^{\cdot}\\ =&2(\dot{u}_N+\dot{u}_{N-1})(u_N-u_{N-2})+4[\dot{u}_N(u_N-u_{N-1})+\dot{u}_{N-1}(u_{N-1}-u_{N-2})]\\ &-\Big[\frac{1}{2}(u_N-u_{N-2})^2+2(u_N-u_{N-1})^2\Big]^{\cdot}.\end{aligned}$$

Noticing the forms of I_1 and I_2, we define

$$\begin{aligned}E_2(t)=&2I_2(N)+4I_1(N)+4I_1(N-1)-\Big[\frac{1}{2}(u_N-u_{N-2})^2\\&+2(u_N-u_{N-1})^2+\frac{1}{2}(u_{-N}-u_{-N+2})^2+2(u_{-N}-u_{-N+1})^2\Big]\\=&4\sum_{k=-N+2}^{N-2}\dot{u}_k^2+\sum_{k=-N+1}^{N-2}(\dot{u}_k+\dot{u}_{k+1})^2+2\dot{u}_{N-1}^2+2\dot{u}_{-N+1}^2\\&+4\sum_{k=-N+1}^{N-2}(u_{k+1}-u_k)^2+\sum_{k=-N+2}^{N-2}(u_{k+1}-u_{k-1})^2\\&+\frac{1}{2}\big[(u_{N-2}-u_N)^2+(u_{-N+2}-u_{-N})^2\big].\end{aligned}\tag{3.6}$$

Then we get

$$\dot{E}_2(t)=-4(u_N-u_{N-2})^2-4(u_{-N}-u_{-N+2})^2\leq 0.\tag{3.7}$$

3.4 Energy functional for MBC3

For MBC3 (2.7c), the calculations are more involved. The procedure is still the same. We first calculate the product of the two sides of (2.7c), and express it as the sum of full derivatives and derivatives in the form of $\dot{u}_K u_{K-k}$. Then we recast them in terms of the derivatives of $I_l(K)$.

More precisely, we calculate

$$\begin{aligned}&(\dot{u}_N+15\dot{u}_{N-1}+15\dot{u}_{N-2}+\dot{u}_{N-3})(3u_N+7u_{N-1}-7u_{N-2}-3u_{N-3})\\=&-\dot{u}_N(38u_{N-1}+52u_{N-2}+6u_{N-3})-\dot{u}_{N-1}(210u_{N-2}+52u_{N-3})-38\dot{u}_{N-2}u_{N-3}\\&+\Big[\frac{3}{2}u_N^2+\frac{105}{2}u_{N-1}^2-\frac{105}{2}u_{N-2}^2-\frac{3}{2}u_{N-3}^2+u_N(45u_{N-1}+45u_{N-2}+3u_{N-3})\\&+u_{N-1}(105u_{N-2}+7u_{N-3})-7u_{N-2}u_{N-3}\Big]^{\cdot}\\=&-20\dot{u}_N(u_N-u_{N-1})+112\dot{u}_{N-1}(u_{N-1}-u_{N-2})-20\dot{u}_{N-2}(u_{N-2}-u_{N-3})\\&+52(\dot{u}_N+\dot{u}_{N-1})(u_N-u_{N-2})+52(\dot{u}_{N-1}+\dot{u}_{N-2})(u_{N-1}-u_{N-3})\\&+6(\dot{u}_N+\dot{u}_{N-2})(u_N-u_{N-1}+u_{N-2}-u_{N-3})\\&+\frac{1}{2}\big[7(u_N-u_{N-1})^2-39(u_N-u_{N-2})^2-59(u_{N-1}-u_{N-2})^2\\&-3(u_N-u_{N-3})^2-7(u_{N-1}-u_{N-3})^2+7(u_{N-2}-u_{N-3})^2\big]^{\cdot}.\end{aligned}$$

Accordingly, we define the following energy functional.

$$\begin{aligned}E_3(t)=&-20I_1(N)+112I_1(N-1)-20I_1(N-2)+52I_2(N)+52I_2(N-1)+6I_3(N)\\&+\frac{1}{2}\Big[7(u_N-u_{N-1})^2-39(u_N-u_{N-2})^2-59(u_{N-1}-u_{N-2})^2\end{aligned}$$

$$
\begin{aligned}
&-3(u_N-u_{N-3})^2-7(u_{N-1}-u_{N-3})^2+7(u_{N-2}-u_{N-3})^2\Big]+n.b.t.\\
=&36\sum_{k=-N+3}^{N-3}\dot{u}_k^2+52\sum_{k=-N+3}^{N-2}(\dot{u}_k+\dot{u}_{k-1})^2+3\sum_{k=-N+3}^{N-1}(\dot{u}_k+\dot{u}_{k-2})^2\\
&+16\dot{u}_{N-1}^2+52\dot{u}_{N-1}\dot{u}_{N-2}+72\dot{u}_{N-2}^2+16\dot{u}_{-N+1}^2+52\dot{u}_{-N+1}\dot{u}_{-N+2}+72\dot{u}_{-N+2}^2\\
&+36\sum_{k=-N+4}^{N-3}(u_k-u_{k-1})^2+52\sum_{k=-N+4}^{N-2}(u_k-u_{k-2})^2\\
&+3\sum_{k=-N+3}^{N}(u_k-u_{k-1}+u_{k-2}-u_{k-3})^2\\
&+\frac{1}{2}\big[-13(u_N-u_{N-1})^2+13(u_N-u_{N-2})^2+33(u_{N-1}-u_{N-2})^2\\
&-3(u_N-u_{N-3})^2+97(u_{N-1}-u_{N-3})^2+79(u_{N-2}-u_{N-3})^2\big]\\
&+\frac{1}{2}\big[-13(u_{-N}-u_{-N+1})^2+13(u_{-N}-u_{-N+2})^2+33(u_{-N+1}-u_{-N+2})^2\\
&-3(u_{-N}-u_{-N+3})^2+97(u_{-N+1}-u_{-N+3})^2+79(u_{-N+2}-u_{-N+3})^2\big].
\end{aligned}
\tag{3.8}
$$

It may be readily checked that $16\dot{u}_{N-1}^2+52\dot{u}_{N-1}\dot{u}_{N-2}+72\dot{u}_{N-2}^2$ is non-negative, so is the negative boundary part. The boundary quadratic terms $3(u_N-u_{N-1}+u_{N-2}-u_{N-3})^2+0.5[-13(u_N-u_{N-1})^2+13(u_N-u_{N-2})^2+33(u_{N-1}-u_{N-2})^2-3(u_N-u_{N-3})^2+97(u_{N-1}-u_{N-3})^2+79(u_{N-2}-u_{N-3})^2]$ may be put into a quadratic form

$$
\frac{1}{2}\begin{bmatrix} u_N & u_{N-1} & u_{N-2} & u_{N-3}\end{bmatrix}\begin{bmatrix} 3 & 7 & -7 & -3\\ 7 & 123 & -39 & -91\\ -7 & -39 & 131 & -85\\ -3 & -91 & -85 & 179\end{bmatrix}\begin{bmatrix} u_N\\ u_{N-1}\\ u_{N-2}\\ u_{N-3}\end{bmatrix}.
$$

The coefficient matrix has four eigenvalues, 0, 1.584, 83.392 and 133.023. So it is non-negative. The other boundary is also non-negative. In conclusion, $E_3(t)$ is non-negative.

Moreover, the above derivations guarantee the dissipation of MBC3 with

$$
\begin{aligned}
\dot{E}_3(t)=&-2(3u_N+7u_{N-1}-7u_{N-2}-3u_{N-3})^2-2(3u_{-N}+7u_{-N+1}-7u_{-N+2}-3u_{-N+3})^2\\
\le&0.
\end{aligned}
\tag{3.9}
$$

3.5 Numerical verifications

We compute over an atomic chain with 201 atoms by the speed verlet algorithm with a time step size $\Delta t=0.01$. Following [13], we take the standard benchmark initial data

$$
u_n(0)=\begin{cases} 0.005[1+0.1\cos(0.4\pi(n-10))]\dfrac{e^{-0.0025(n-101)^2}-e^{-6.25}}{1-e^{-6.25}}, & 51<n<151,\\ 0, & \text{elsewhere.}\end{cases}
\tag{3.10}
$$

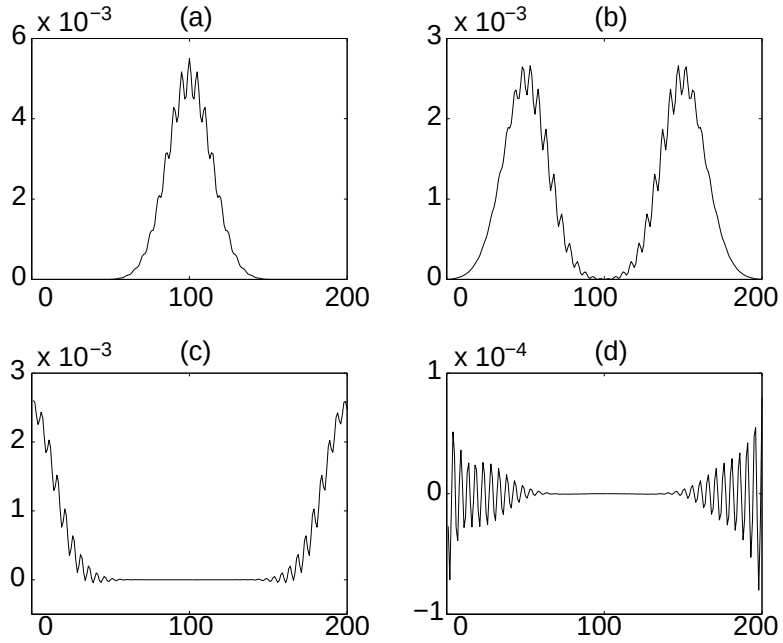

Figure 2: Snapshots of atomic motion: (a) $u_n(0)$; (b) $u_n(50)$; (c) $u_n(100)$; (d) $u_n(150)$. The horizontal axis represents the atomic numbering, and the vertical axis represents the displacement.

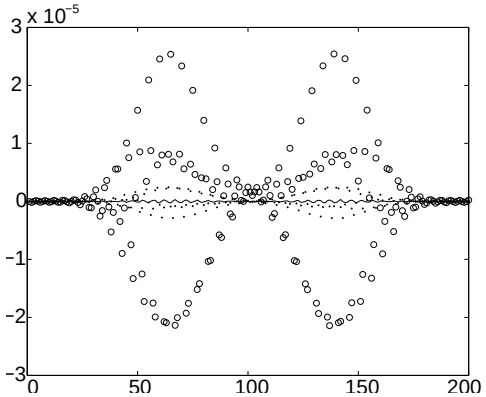

Figure 3: Comparison of $u_n(200)$ with different boundary conditions: circles for MBC1, dots for MBC2, and solid curve for MBC3. The horizontal axis represents the atomic numbering, and the vertical axis represents the displacement.

The velocity is uniformly zero initially. The evolution is depicted in Fig. 2, where MBC1 is adopted for boundary treatment. The evolution is essentially the same when the other two MBC's are used, but the reflection is considerably reduced. See Fig. 3. In fact, at $t = 200$, the amplitude of the reflected wave with MBC3 is about 1% that with MBC1. Moreover, it is observed that $u_n(200)$ with MBC1 contains oscillations corresponding to considerably larger components of shortwaves. In contrast, the shortwaves are well re-

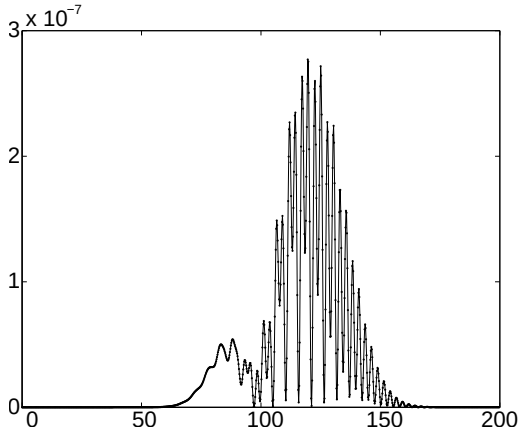

Figure 4: Energy decay rate for MBC1: solid curve for numerically calculated $-\dot{E}_1(t)$ and dots for $2(u_N-u_{N-1})^2+2(u_{-N}-u_{-N+1})^2$. The horizontal axis represents time, and the vertical axis represents the rate.

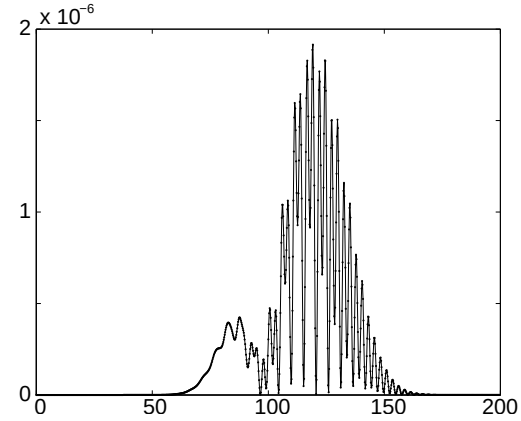

Figure 5: Energy decay rate for MBC2: solid curve for numerically calculated $-\dot{E}_2(t)$ and dots for $4(u_N-u_{N-2})^2+4(u_{-N}-u_{-N+2})^2$. The horizontal axis represents time, and the vertical axis represents the rate.

solved by MBC3. This agrees with the previous study of reflection coefficients for these three boundary conditions.

The energy decay rates are depicted in Figs. 4, 5 and 6, respectively. The numerically calculated decay rate and the one calculated by the boundary terms coincide almost exactly in each case. The theoretical results are thus verified. We notice that the energy decay profiles are almost exactly the same for three boundary conditions, except for different scales resulted from the definition of the energy functionals. The data shown in these figures are basically during the stage when the wave propagates outward and through the boundaries for the first time. The differences in these three boundary conditions become observable when the reflected waves propagate across the boundaries for a second time, which are in an even smaller scale. These are indicated from the comparison of reflected waves at $t=200$ in Fig. 3.

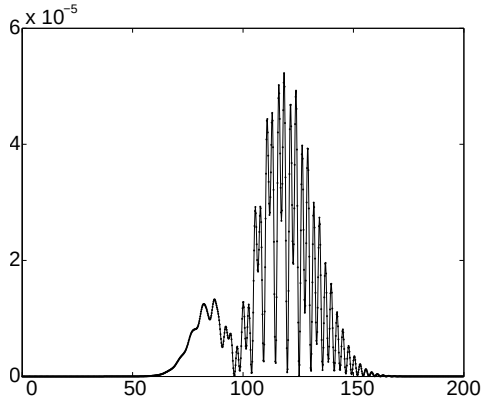

Figure 6: Energy decay rate for MBC3: solid curve for numerically calculated $-\dot{E}_3(t)$ and dots for $2(3u_N+7u_{N-1}-7u_{N-2}-3u_{N-3})^2+2(3u_{-N}+7u_{-N+1}-7u_{-N+2}-3u_{-N+3})^2$. The horizontal axis represents time, and the vertical axis represents the rate.

4 Stability of MBC1 for a nonlinear chain

We consider a nonlinear chain, for which the pairwise potential reduces to be quadratic for $|k|\geq N$, namely, $J_{k-1/2}(u_k-u_{k-1})=(u_k-u_{k-1})^2/2$. The Newton equations are

$$\ddot{u}_k=J'_{k+1/2}-J'_{k-1/2},\quad k\in\mathbb{Z}. \tag{4.1}$$

The right hand side becomes $u_{k-1}-2u_k+u_{k+1}$ for $|k|\geq N$.

Let the energy functional be

$$\tilde{E}_1(t)=\sum_{k=-N+1}^{N-1}\dot{u}_k^2+2\sum_{k=-N+2}^{N-1}J_{k-1/2}+\frac{1}{2}(u_{-N}-u_{-N+1})^2+\frac{1}{2}(u_N-u_{N-1})^2. \tag{4.2}$$

Direct calculations show that

$$\begin{aligned}\dot{\tilde{E}}_1(t)=&2\sum_{k=-N+1}^{N-1}\dot{u}_k(J'_{k+1/2}-J'_{k-1/2})+2\sum_{k=-N+2}^{N-1}J'_{k-1/2}(\dot{u}_k-\dot{u}_{k-1})\\&+(u_{-N}-u_{-N+1})(\dot{u}_{-N}-\dot{u}_{-N+1})+(u_N-u_{N-1})(\dot{u}_N-\dot{u}_{N-1})\\=&-2\dot{u}_{-N+1}J'_{-N+1/2}-2\dot{u}_{N-1}J'_{N-1/2}\\&+(u_{-N}-u_{-N+1})(\dot{u}_{-N}-\dot{u}_{-N+1})+(u_N-u_{N-1})(\dot{u}_N-\dot{u}_{N-1})\\=&-2(u_{-N}-u_{-N+1})^2-2(u_N-u_{N-1})^2\\\leq&0.\end{aligned}$$

5 Discussions

Stability for atomic chains is an important issue, yet difficult to establish in general. There are extensive studies for continuous systems, as well as the von Neumann analysis for

finite difference method of the Cauchy problem for general linear systems. However, they do not directly apply to discrete initial boundary value problems. A general effective methodology is still not available, and specific problems need specific treatment to construct energy functionals, e.g., [19]. We notice that for the discrete dynamical systems, one may investigate the stability by either the Lyapunov method, or the corresponding eigenvalue problem in case of a linear system. However, a rigorous proof of non-positive eigenvalue involves the theory of polynomial equations, which is not available as the degree is high. The construction of Lyapunov function is not an easy task, particularly with the delicacy arising from the fact that accurate boundary treatments like MBC are usually dissipation-free or with very weak dissipation. Accordingly, there is usually a zero eigenvalue. This makes the system marginally stable, and theoretical stability proof important and difficult.

In this paper, we have constructed explicitly the energy functionals for three MBC's in a linear atomic chain. They bear similar features to a Lyapunov function, except inducing semi-norms rather than norms. Consequently, the atomic simulations equilibrate up to a dilation. The construction consists of four steps. First, we study some elemental functionals and their derivatives. Secondly, we express terms in the form of $\dot{u}_K u_{K-l}$ in terms of these functional derivatives and a complete derivative. Thirdly, we compute the product of the two sides in a boundary condition. Finally, according to the form of resulting functional derivatives and complete derivatives, we construct a functional to establish the stability. This method may apply to more general boundary conditions for the harmonic lattice and linear lattices with non-nearest neighbor interaction. However, in case of nonlinear systems, we have only worked out the stability for MBC1. Further explorations are desirable.

Acknowledgements

This study is supported in part by NSFC under contract number 11272009, National Basic Research Program of China under contract number 2010CB731503. We would like to thank the anonymous reviewers for their valuable suggestions.

References

[1] S. A. ADELMAN AND J. D. DOLL, *Generalized Langevin equation appraoch for atom/solid-surface scattering: collinear atom/harmonic chain model*, J. Chem. Phys., 61 (1974), pp. 4242–4245.

[2] W. CAI, M. DE KONING, V. V. BULATOV AND S. YIP, *Minimizing boundary reflections in coupled-domain simulations*, Phys. Rev. Lett., 85 (2000), pp. 3213–3216.

[3] M. DREHER AND S. TANG, *Time history interfacial conditions in multiscale computations of lattice oscillations*, Comput. Mech., 41 (2008), pp. 683–698.

[4] M. FANG, Boundary Treatments and Statistical Convergence of Particle Simulations, PhD Thesis, Peking University, Beijing, 2012.

[5] M. FANG, S. TANG, Z. LI AND X. WANG, *Artificial boundary conditions for atomic simulations of face-centered-cubic lattice*, Comput. Mech., 50 (2012), pp. 645–655.
[6] M. FANG, X. WANG, Z. LI AND S. TANG, *Matching boundary conditions for scalar waves in face-centered-cubic lattice*, Adv. Appl. Math. Mech., 5 (2013), pp. 337–350.
[7] E. G. KARPOV, H. S. PARK, W. K. LIU AND D. L. DOROFEEV, *On the modelling of chaotic thermal motion in solids*, Preprint.
[8] W. K. LIU, E. G KARPOV AND H. S. PARK, Nano-Mechanics and Materials: Theory, Multiscale Methods and Applications, Wiley, 2005.
[9] G. PANG AND S. TANG, *Time history kernel functions for square lattice*, Comput. Mech., 48 (2011), pp. 699–711.
[10] S. SAVADATTI AND M. GUDDATI, *Absorbing boundary conditions for scalar waves in anisotropic media, part 1: time harmonic modeling*, J. Comput. Phys., 229 (2010), pp. 6696–6714.
[11] S. TANG, *A finite difference approach with velocity interfacial conditions for multiscale computations of crystalline solids*, J. Comput. Phys., 227 (2008), pp. 4038–4062.
[12] S. TANG AND M. FANG, *Unstable surface modes in finite chain computations: deficiency of reflection coefficient approach*, Commun. Comput. Phys., 8 (2010), pp. 143–158.
[13] S. TANG, T. Y. HOU AND W. K. LIU, *A mathematical framework of the bridging scale method*, Int. J. Numer. Methods Eng., 65 (2006), pp. 1688–1713.
[14] S. TANG, T. Y. HOU AND W. K. LIU, *A pseudo-spectral multiscale method: interfacial conditions and coarse grid equations*, J. Comput. Phys., 213 (2006), pp. 57–85.
[15] L. N. TREFETHEN, *Stability of finite-difference models containing two boundaries or interfaces*, Math. Comput., 45 (1985), pp. 279–300.
[16] A. TO AND S. LI, *Perfectly matched multiscale simulations*, Phys. Rev. B, 72 (2005), 035414.
[17] G. J. WAGNER AND W. K. LIU, *Coupling of atomistic and continuum simulations using a bridging scale decomposition*, J. Comput. Phys., 190 (2003), pp. 249–274.
[18] X. WANG AND S. TANG, *Matching boundary conditions for lattice dynamics*, Int. J. Numer. Methods Eng., 93 (2013), pp. 1255–1285.
[19] W. YONG AND Y. ZHU, *Convergence of finite difference method for nonlinear movable boundary problem*, Science in China, Series A, 8 (1989), pp. 785–795 (in Chinese).